Nuclear Instruments and Methods in Physics Research A270 (1988) 334–346
North-Holland, Amsterdam

RESULTS FROM A TEST OF AN IRON STREAMER TUBE CALORIMETER

H1 Collaboration

W. BRAUNSCHWEIG, H. GENZEL, F.J. KIRSCHFINK, M. RÖHNER, J. TUTAS and E. VOGEL
I. Physikalisches Institut der RWTH Aachen, FRG *

M. WIDGOFF
Department of Physics, Brown University, Providence, USA

F.W. BRASSE, W. FLAUGER, J. GAYLER, V. KORBEL, J. MARKS and Ch. ZEITNITZ
Deutsches Electronen Synchrotron, DESY, Hamburg, FRG

F. BRINKER, S. BRINKMANN, P. HARTZ, K. RAUSCHNABEL, A. WALTHER and D. WEGENER
Institut für Physik, Universität Dortmund, FRG **

E. BARRELET [+], V. BRISSON, D. LELLOUCH [++], P. PERRODO and C. VALLÉE
Ecole Polytechnique, Palaiseau, France

A.J. CAMPBELL
University of Glasgow, UK

H.T. BLUME [§], K. LAU, F. LIPP and R. WEINSTEIN
Department of Physics, University of Houston, USA

H. GREIF, J. HUBER, C. KIESLING [§§], D. LÜERS, H. OBERLACK and P. SCHACHT
Max-Planck-Institut für Physik und Astrophysik, München, FRG

E. von GOELER and J. MOROMISATO
Department of Physics, Northeastern University, Boston, USA

B. DELCOURT and A. JACHOLKOWSKA
Laboratoire de l'Accélérateur Linéaire, Orsay, France

J. DUBOC and H. NGUYEN
Laboratoire de la Physique Nucléaire et Hautes Energies, Université de Paris, France

V. BIDOLI, F. FERRAROTTO and B. STELLA
INFN e Università di Roma "La Sapienza", Italy

* Supported by the German Bundesministerium für Forschung und Technologie under contract number 054AC17P.
** Supported by the German Bundesministerium für Forschung und Technologie under contract number 054DO057I.
[+] Now at Université de Paris, France.
[++] Now at Weizmann Institute of Science, Israel.
§ Now at Max-Planck-Institut für Physik and Astrophysik, München, FRG.
§§ Heisenberg-Stipendiat der Deutschen Forschungsgemeinschaft.

0168-9002/88/$03.50

M. BESANÇON, G. COZZIKA, M. DAVID, J. FELTESSE, A. DE LESQUEN, P. VERRECCHIA and G. VILLET

Centre d'Études Nucléaires, Saclay, France

U. STRAUMANN

Physikalisches Institut der Universität Zürich, Switzerland

Received 12 February 1988

We have measured the response and energy resolution of an iron streamer tube calorimeter with 7.5 cm sampling for pions in the energy range from 10 to 100 GeV. For fully contained events, the energy resolution can be described by $\sigma_E/E \approx 100\%/\sqrt{E}$.

1. Introduction

The H1 experiment [1] foreseen at the e–p storage ring HERA will use limited streamer tubes for the instrumentation of the iron yoke. These tubes will serve as active elements of the muon detector and calorimeter for hadrons which penetrate through the central liquid argon (LAr) hadron calorimeter. We have measured the response of a prototype streamer tube calorimeter both in a stand-alone mode and behind a LAr hadron calorimeter. The aim of the test was threefold: (1) to gain experience with streamer tubes under beam conditions, (2) to study the performance of the proposed detector scheme and (3) to compare the Monte Carlo simulation parameters with the measurements. In this paper we report on the stand-alone test of the streamer tube calorimeter. Results on the performance of the LAr calorimeter have been given in ref. [2]. The results of the combined test will be given in a forthcoming paper [3].

2. Experimental setup

2.1. Beam and beam detectors, trigger and data acquisition

The test calorimeter was exposed to pions and muons ($10 \leq p \leq 100$ GeV/c) provided by the H6 beam [4] of the SPS at CERN. The beam was run in the tertiary mode [5]. For momenta $p \leq 50$ GeV/c, pions were separated from electrons by two Cherenkov counters with ring selection (CEDARs) [6]. The typical momentum spread of the beam was $\Delta p/p = 0.8\%$. Further details are given in ref. [2].

The layout of the experimental area is shown in fig. 1. In front of the streamer tube calorimeter, two multiwire proportional chambers (MWPCs) with an active area of 25×25 cm^2 were installed. The distance between the two chambers was 19 cm. Each one consisted of a horizontal and a vertical anode plane. The wire

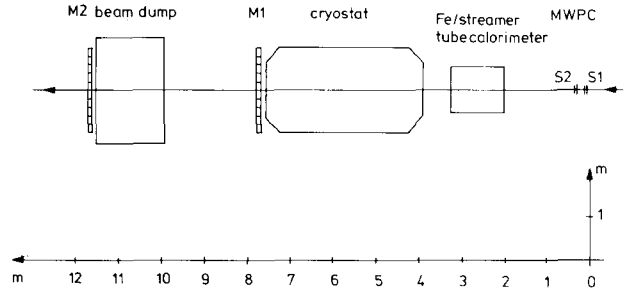

Fig. 1. Schematic view of the test setup.

spacing was 2 mm. The MWPCs were covered by scintillation counters on both sides (S1 and S2). The streamer tube calorimeter was installed in front of the LAr calorimeter [2] which was not read out. Behind the LAr calorimeter (depth about 10 nuclear interaction lengths (λ)) and behind the beam dump (1.6 m iron), two scintillator hodoscopes for muon detection were installed (M1 and M2). Each consisted of 10 vertically oriented counters of 120 cm height and 20 cm width with an overlap of 0.5 cm between two adjacent counters.

The MWPC and the scintillators S1 and S2 were used for the trigger. The signals of the muon walls M1

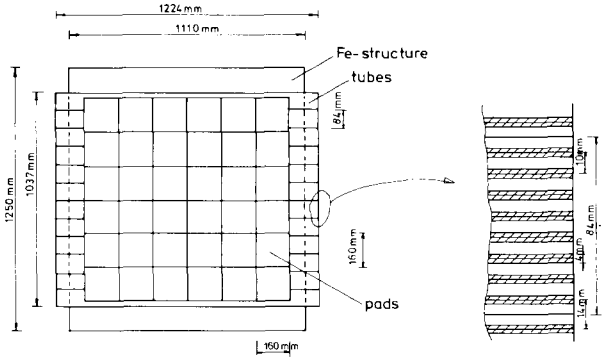

Fig. 2. Front view of the test detector.

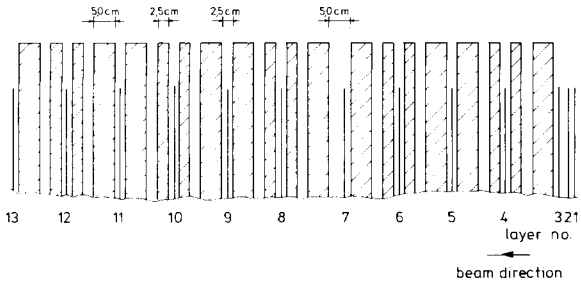

Fig. 3. Side view of the test detector.

and M2 were recorded for offline muon selection. The data acquisition system is described in ref. [2].

2.2. The test detector

The test detector used iron as absorber (75 cm in total, 4.47λ) and wire chambers which were operated in the limited streamer mode as active detector elements. Schematic side and front views of the detector are shown in figs. 2 and 3.

The detector consisted of 10 iron plates of 5.0 cm thickness and 10 iron plates of 2.5 cm thickness. The actual sampling used was 7.5 cm, which is equal to the one foreseen for the H1 detector [1]. The gaps between the plates were 2.5 cm wide except after 30 cm of iron where the gap width was 5.0 cm. The lateral dimensions of the stack were 110×125 cm^2.

The detector was equipped with a total of 13 chamber planes. Each plane consisted of twelve PVC streamer tube elements of the Iarocci type [7] without cover [8], 156 elements in total. The details of the tube elements are shown in fig. 4. The length of the elements was 120 cm. The surface resistivity of the cathode, R_s, was in the range of 100 k$\Omega/\Box \leq R_s \leq 1$ M$\Omega/\Box$. In total, 243 elements were fabricated at the INFN Frascati. Before installing them into the detector, a 24 h high voltage test was performed. Tube elements which drew currents larger than 2 μA at 4.7 kV after this test were rejected (in total 25 elements). The remainder were used to instrument the detector.

The readout was done with pickup electrodes. On the coverless side, the tubes were equipped with strips

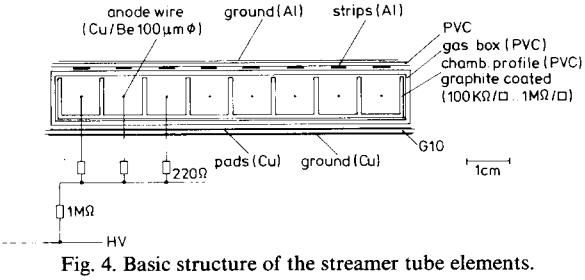

Fig. 4. Basic structure of the streamer tube elements.

Table 1
Location of the different layers in the test detector

Layer number	Iron depth [cm]	Equipped with			Tower number
		pads	parallel strips	orthogonal strips	
1	0.0		*	*	
2	0.0		*	*	
3	0.0	*	*		presampler
4	7.5	*	*		1
5	15.0	*	*		1
6	22.5	*	*		1
7	30.0	*	*		1
8	37.5	*	*		1
9	45.0	*	*		2
10	52.5	*	*		2
11	60.0	*	*		2
12	67.5	*	*		2
13	75.0	*			2

parallel to the wire (all layers except 3 and 13), whereas the covered side was equipped either with orthogonal strips (layers 1 and 2) or pads (all other layers), as shown in fig. 3 and table 1 (except for three missing muon chamber layers, this scheme is equal to the one originally foreseen for the H1 detector). The total active area was about 1 m^2. The wires were oriented horizontally. All layers were aligned in the vertical direction except layer 2 which was shifted upwards by 0.5 cm to achieve full geometric acceptance for the double layer. The width of the strips was 4 mm with a pitch of 1 cm, in total 96 strips per layer. The readout of the strips was performed by the streamer tube operating systems STOS of LeCroy Research Systems Corporation (LRS) *. The pad size was 16×16 cm^2 (6×6 pads per layer). The pads of layer 3 were read out seperately (presamplers), whereas the consecutive pads of layers 4, 5, 6, 7 and 8 (9, 10, 11, 12 and 13) were added to form the first (second) towers, as foreseen for H1. The pad signals were fed into a special electronic device where the towers were formed: the signals were summed up and inverted with a gain of 1.0 for the presamplers and 0.1 for the towers. A block diagram of the pad readout is shown in fig. 5. The output signals were digitized using LRS 2249A ADCs (10-bit resolution, 0.25 pC per channel sensitivity). The integration time of the ADCs was 200 ns. All electronics was located close to the detector.

* About 10% of the electronic STOS channels were broken. As the STOS electronics is no longer supported by LRS, the broken channels could neither be repaired nor replaced. They were mainly placed at the edge of the detector. Within the region of ± 10 cm around the beamline (in this region, for hadron showers, about 80% of the energy is deposited), only 3% of the channels were broken.

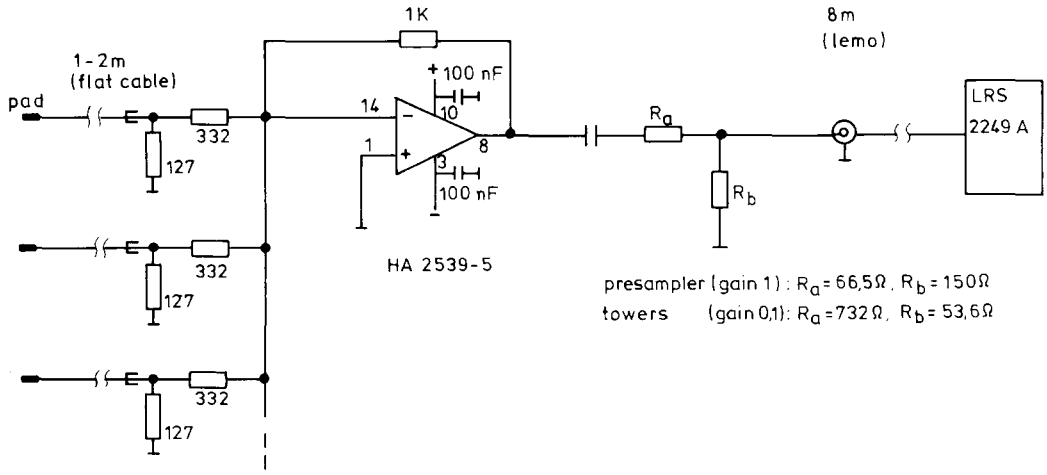

Fig. 5. Block diagram for pad readout.

Table 2
Number of electronic channels used

Type	Number of channels per layer	Number of layers	Total
Analog (pads)	6×6	3	108
Digital (parallel strips)	96	11	1056
Digital (orthogonal strips)	96	2	192
Digital (sum)	96	13	1248

The total number of readout channels is listed in table 2.

The high voltage was fed into the tubes via a 1 MΩ resistor per tube and a 220 Ω resistor inside the tubes for each wire (see fig. 4). The chambers were operated at high voltages of 4.7 and 4.6 kV. The gas mixture used was 25% argon and 75% isobutane.

3. Results

3.1. Results for incident muons

The muon analysis was done with data from three sources:

(1) After the transportation to CERN, the detector was set up in a parking position behind the beam dump, where the status of the apparatus was checked and the high voltage efficiency plateau curve (see section 3.1.1) was measured. In this position, we used a special trigger and data acquisition system which allowed only an on-line analysis. The data consisted of a mixture of cosmic muons and beam muons. After these tests the detector was moved into the beam.

(2) Before and after the running period, the data taken in special beam runs using M1 and M2 as trigger were written to tape. These data were mainly used for the intercalibration of the towers (see section 3.2.2).

(3) From the data taken in normal hadronic beam runs, muons were selected off-line. These data were used for the detailed studies of the detector response to muons (see section 3.1.2).

3.1.1. High voltage efficiency plateau curve

The dependence of the chamber efficiency for strip readout (averaged over all planes) on the high voltage (HV) and the readout threshold * applied is shown in fig. 6. It was measured on-line using the special muon trigger mentioned above. The algorithm for the on-line program was similar to the one described in section 3.1.2, except that a special treatment of dead channels in the digital electronics was not included. The absolute values of the efficiencies are different from the ones given below because of the different beam conditions and because of the dead channels in the digital electronics. From the data of fig. 6, we decided to operate the detector at a high voltage of 4.7 kV and a nominal threshold of 50 mV.

For high muon rates (≥ 20 Hz/cm^2), we observed dark currents of about 2 μA in some of the chambers. This problem was less severe at lower high voltage. In order to study the performance of the detector if the high voltage has to be reduced due to large backgrounds, a part of the pion data was also taken at a high voltage of 4.6 kV and a nominal threshold of 50 mV.

* The thresholds are defined by an external reference voltage between −30 and +2000 mV, corresponding to a signal current threshold between 30 and 200 μA.

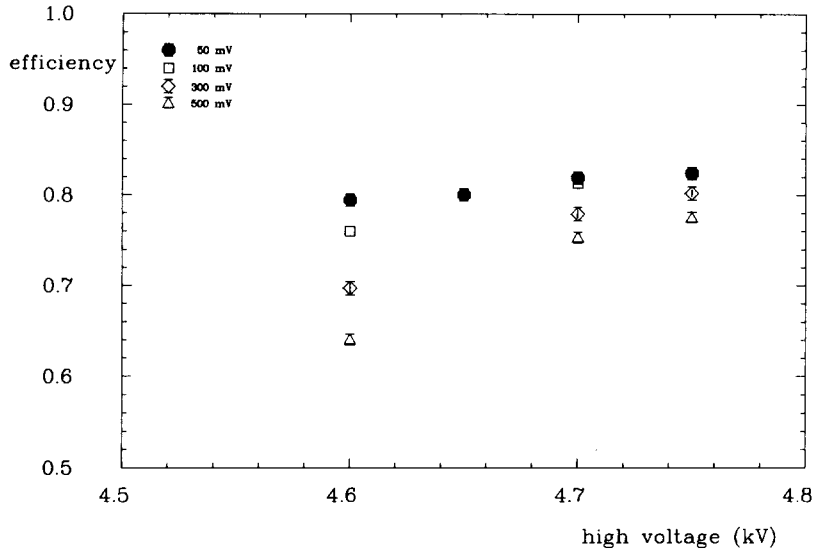

Fig. 6. Chamber efficiency (from strip readout) for different readout thresholds vs high voltage.

3.1.2. Strip and pad response for muons

During the pion runs, no special muon trigger was incorporated. The signals of the muon walls M1 and M2 were, however, recorded and could be used for off-line muon selection. The following cuts were used:

(1) Muon walls: one or two of the central counters of M1 and M2 fired.
(2) MWPC: exactly one cluster in each of the four planes of the MWPC.
(3) Hit pattern in the calorimeter: exactly one cluster of arbitrary size in at least one of the layers of each of the following groups: (1, 2, 4), (5, 6), (7, 8), (9, 10) and (11, 12).

With these cuts, a sample of about 9300 muons at 4.7 kV and about 8600 muons at 4.6 kV remained.

The efficiency and cluster size in each plane was obtained by using all other planes as independent tracking system. In addition, no dead channels in the digital electronics were allowed in the region of the cluster. Efficiencies and mean cluster sizes for 4.7 and 4.6 kV are given in table 3. As the walls of all chamber layers except layer 2 were aligned within about 1 mm, the inefficiencies due to the chamber walls are not fully included in this measurement, such that the measured efficiency is somewhat higher than expected from the geometric inefficiency of about 10%. The multiplicity

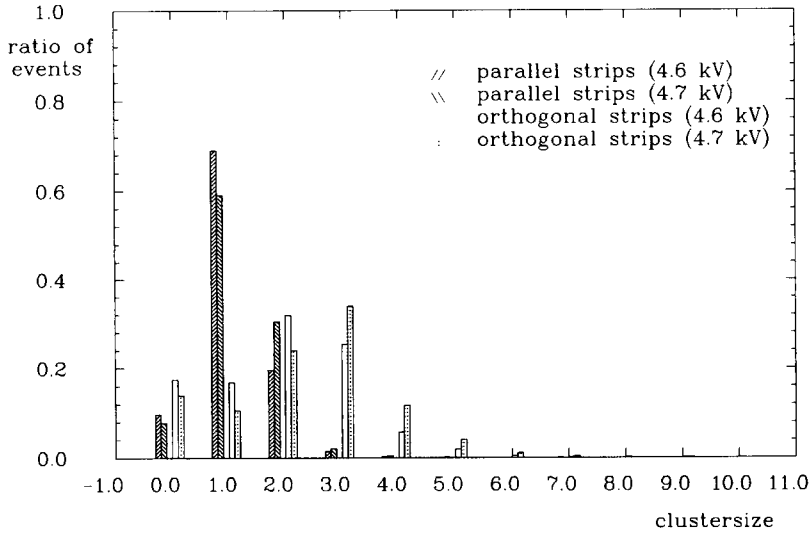

Fig. 7. Strip multiplicity per cluster for muons. Shown are the distributions for parallel and orthogonal strips for 4.6 and 4.7 kV.

Table 3
Mean multiplicities and efficiencies per layer for parallel and orthogonal strips for muon events at 4.7 and 4.6 kV

High voltage	4.7 kV	4.6 kV
Parallel strips:		
Mean multiplicity/layer	1.292 ± 0.002	1.140 ± 0.002
Efficiency/layer	(92.2 ± 0.1)%	(90.3 ± 0.1)%
Orthogonal strips:		
Mean multiplicity/layer	2.385 ± 0.020	1.945 ± 0.018
Efficiency/layer	(86.0 ± 1.3)%	(82.6 ± 0.5)%

distribution per cluster is shown in fig. 7 for parallel and orthogonal strips at high voltages of 4.7 and 4.6 kV. At 4.7 kV, the mean multiplicity for the parallel strips is 1.3, whereas for the orthogonal strips the multiplicity is larger (2.4) and the efficiency is lower. This is due to the fact that (1) the signals on the parallel strips are larger than on the orthogonal strips because the parallel strips are on the coverless side of the tubes, whereas the orthogonal strips are on the graphited side and (2) for the parallel strips, the streamer position is always close to the center of the strip, which is not generally true for the orthogonal strips. Thus a streamer generally illuminates one parallel strip, but more than one orthogonal strip. The total strip multiplicity for the parallel strips is given in fig. 8. As expected from the mean cluster size, the total mean is close to the number of planes used (10).

The pad spectra were obtained from the selected muon events in the following way: After pedestal substraction, a readout threshold of $2\sigma_{rms}$ of the noise distribution was applied to each tower. This corresponds to about 10 pC primary charge or half the charge of a single streamer (see below). The signals of the central four pads of the first and second tower were added to get the total spectrum. Fig. 9 shows these spectra for 4.7 and 4.6 kV. The peak value is 185 (145) pC at 4.7 (4.6) kV with a resolution of $\sigma_{rms}/\text{peak} \approx 43\%$. Assuming a mean value of 9 streamers for a penetrating muon (10 planes with 90% efficiency each), this results in a measured charge of 20.6 (16.1) pC per streamer. Due to instabilities of the gas system and due to rate effects, the muon signal varied with time within $\pm 12\%$. This variation was permanently monitored and the pion data were corrected accordingly.

On those groups of pads which were located above the same tube element, we observed a negative cross-talk. Fig. 10a shows the correlation between the signal on a pad hit by a muon versus the signal on the other pads located above the same tube element (i.e. with the same vertical coordinate). A correlation of about -9% is seen. The same plot for pads perpendicular to the wire direction (i.e. with the same horizontal coordinate) is shown in fig. 10b. No correlation is seen. In this case,

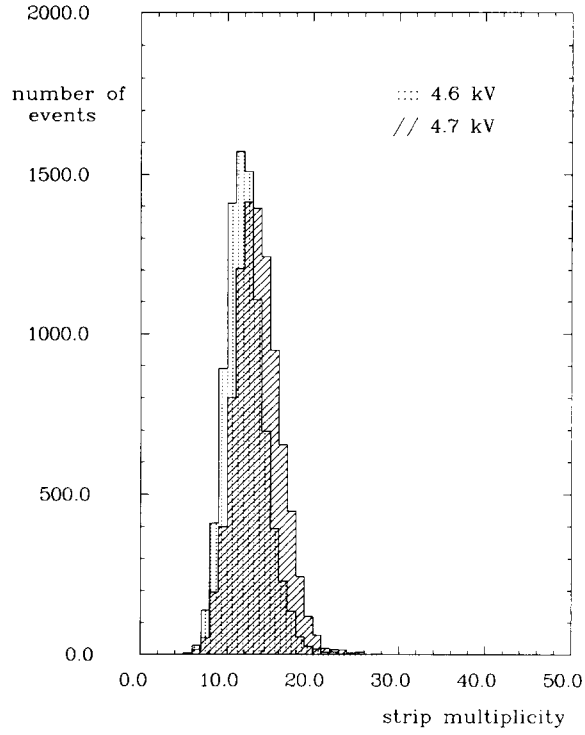

Fig. 8. Total strip multiplicity (parallel strips only) for muons at 4.6 and 4.7 kV.

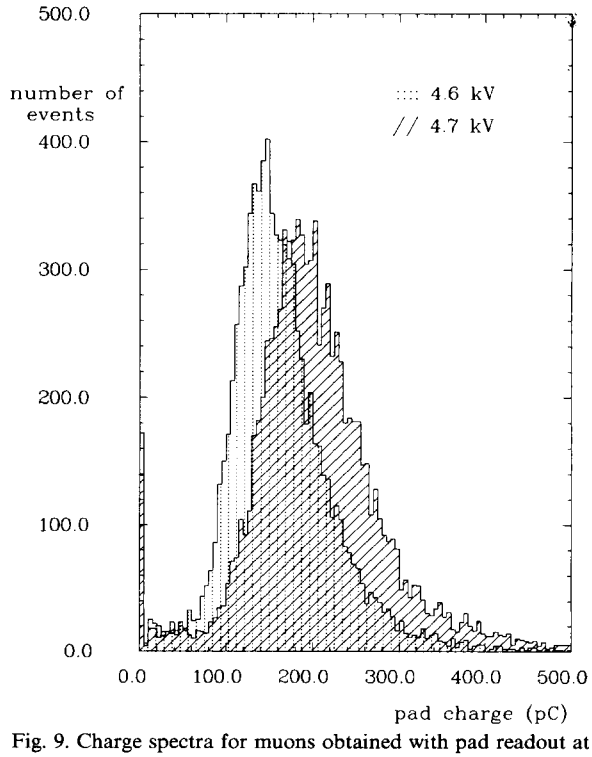

Fig. 9. Charge spectra for muons obtained with pad readout at 4.6 and 4.7 kV.

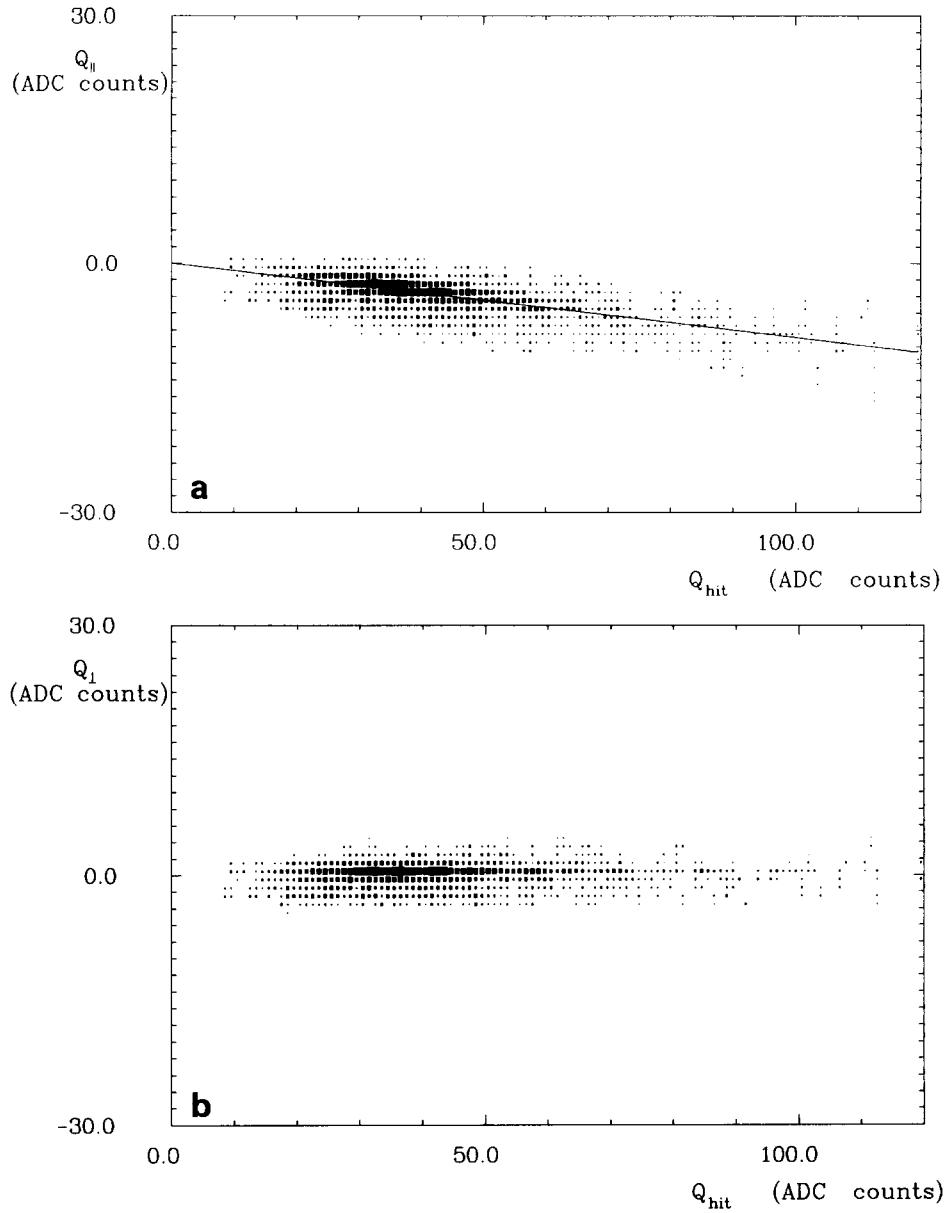

Fig. 10. Crosstalk observed on the pads: (a) in wire direction: signal on neighbouring pads located above the hit wire ($Q_{\parallel}$) vs signal on hit pad (Q_{hit}), together with -9% line; (b) perpendicular to the wire direction: signal on neighbouring pads perpendicular to the wire direction ($Q_{\perp}$) vs signal on hit pad (Q_{hit}).

the signal on the other pads is compatible with noise. Similar effects have been observed by other groups [9].

3.2. Results for incident pions

3.2.1. Event selection

Beside the trigger condition, the following cuts were applied to select pion events:

(1) CEDARs: the beam particle must have been positively identified as a pion by at least one of the two Cherenkov counters.

(2) Muon walls: no hits in M1 and M2.

(3) MWPC: exactly one cluster in each of the four planes of the MWPC,

(4) First chamber layer: in layers 1 and 2 in front of the first iron section at most one cluster was allowed with at most 3 (6) parallel (orthogonal) strips.

Cuts (1) and (2) are used for particle identification,

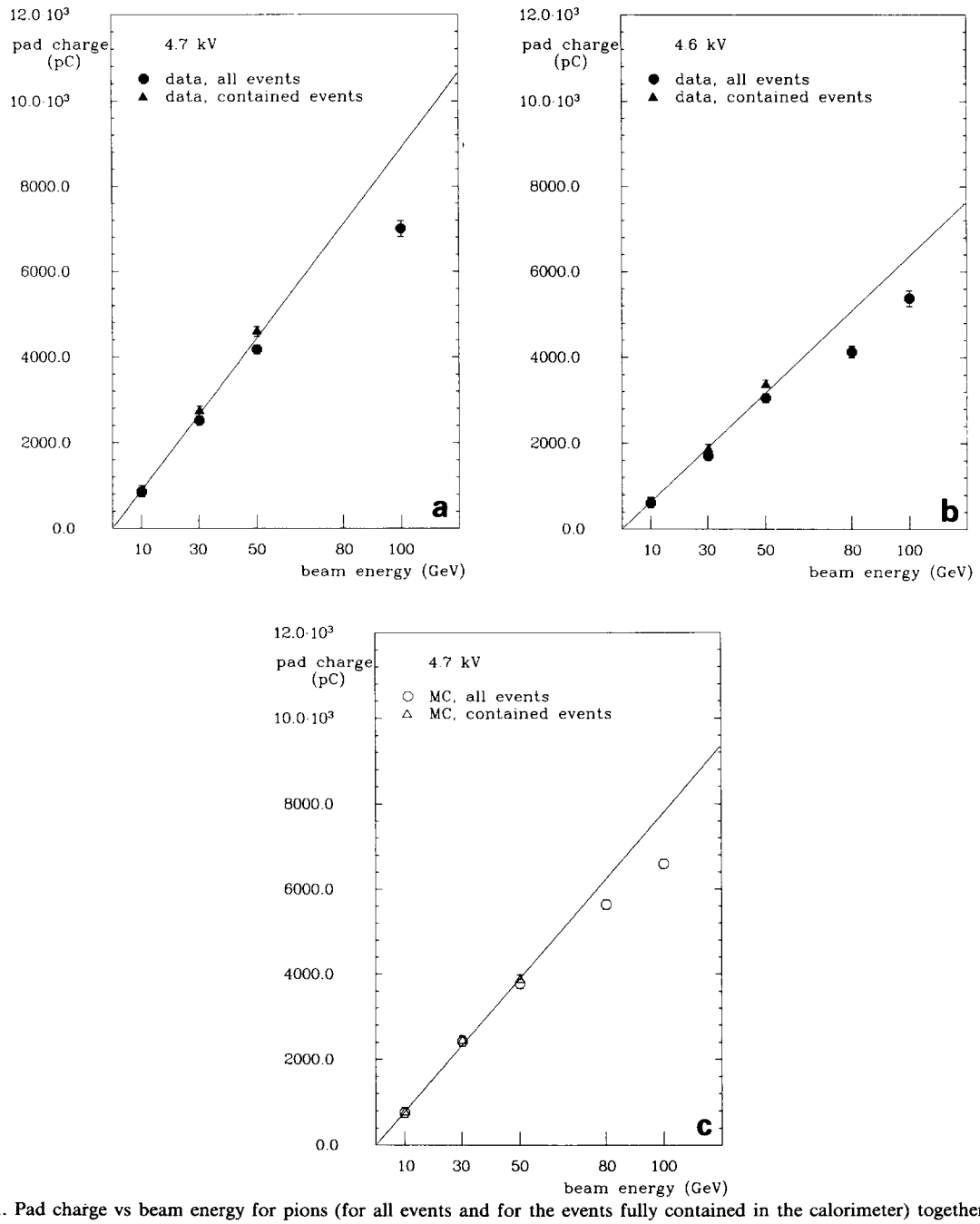

Fig. 11. Pad charge vs beam energy for pions (for all events and for the events fully contained in the calorimeter) together with a straight line fit to the contained event data for (a) 4.7 kV (data, (b) 4.6 kV (data), (c) 4.7 kV (Monte Carlo).

whereas cuts (3) and (4) ensure that exactly one beam particle enters the test detector. Table 4 gives the total number of events obtained after these cuts. For beam energies of 10, 30 and 50 GeV the electron rejection of the CEDARs (the probability to accept an electron as a pion is of the order of 10^{-4}) yields a clean pion sample. For 80 and 100 GeV, however, an electron contamination of about 3% for both energies was observed. This was estimated from the different longitudinal shower profiles for electrons and pions.

To study the influence of longitudinal leakage, we selected events with no fired strip in the last chamber layer equipped with strips (layer 12). This cut implies full containment of the showers within 4.1λ. Due to the

Table 4
Total number of accepted pion events, number of events remaining after the containment cut and reduction factor of the containment cut for the different beam energies and high voltage

Beam energy [GeV]	All events		Contained events		Reduction factor
	4.7 kV	4.6 kV	4.7 kV	4.6 kV	
10	20239	20599	12452	13266	0.63
30	43121	33621	10122	8645	0.24
50	11552	9217	1368	1147	0.12
80	0	10691			
100	8437	9568			

electron contamination of the 80 and 100 GeV data, this cut was only used for the low energy runs. The numbers of events and the rejection factor obtained with this cut are also given in table 4.

Most of the results given in this section have been obtained at a high voltage of 4.7 kV (if not mentioned differently). Some results will also be given for 4.6 kV.

3.2.2. Energy measurement using the pads

After pedestal subtraction, a readout threshold of $2\sigma_{\text{rms}}$ of the noise distribution was applied to each tower (see section 3.1.2). The different towers were intercalibrated using muons. These muons were taken in special runs before and after the running period. For the central four pads of the first and second tower, the calibration values differ by $\pm 5\%$. The improvement on the energy resolution obtained by the intercalibration is, however, insignificant. A correction for the negative crosstalk mentioned in section 3.1.2 was not done for the following reasons: (1) the ADCs were unipolar and thus not able to measure the negative crosstalk for beam energies ≥ 30 GeV properly and (2) since the lateral shower width extends to only two towers and the crosstalk is about constant, it should not affect the energy resolution, but mainly the absolute calibration. This has been verified by Monte Carlo simulations. The total charge for each event was obtained by adding the measured charge in each channel above threshold in the first and second tower. Finally, to correct for variations in the gas amplification, the total measured charge was normalized to the mean muon signal for each run. Fig. 11a shows the linearity curves both for all events and for the events fully contained in the calorimeter. For the contained events, good linearity is obtained up to 50 GeV. If one includes all events, a decrease of the signal is observed ($\sim 8\%$ at 30 GeV, $\sim 10\%$ at 50 GeV). For the highest energies, the signal is further reduced due to ADC overflows. This effect was estimated to about -7% at 100 GeV [10]. Using the contained events, an absolute calibration of (88.9 ± 0.9) pC/GeV is obtained. Taking the mean charge per streamer as measured with muons (see section 3.1.2) and neglecting the influence of the negative crosstalk, this corresponds to 4.3 streamers per GeV incident energy.

Energy resolutions have been obtained from the charge spectra with a Gaussian fit in the region

$$\langle Q \rangle - 2\sigma_{\text{rms}} \leq Q \leq \langle Q \rangle + 2\sigma_{\text{rms}},$$

where $\langle Q \rangle$ and σ_{rms} are the mean value and the rms resolution of the charge spectrum after the rejection of the tails of the distribution. For the 10 GeV data, additionally the region

$$Q \leq \langle Q^{\mu} \rangle + 1.5\sigma^{\mu}_{\text{rms}}$$

was left out of the fit, where $\langle Q^{\mu} \rangle$ and $\sigma^{\mu}_{\text{rms}}$ are the mean value and the rms resolution of the charge spectrum for muons. Fig. 12 shows the charge spectrum both for all events and for the contained events at 30 GeV together with a Gaussian fit. The resolution σ_Q/Q obtained by this procedure both for all events and for the fully contained events (only for $E_{\text{beam}} \geq 50$ GeV, see section 3.2.1) are shown in fig. 13a. For the fully contained events, the resolution can be described by

$$\sigma_E/E \approx 100\%/\sqrt{E}$$

(full line fig. 13a), whereas the decrease of the resolution is slower than $\sim 1/\sqrt{E}$ due to leakage when all events are included. In the case of H1, the effect of leakage will be much less severe, since in the H1 detec-

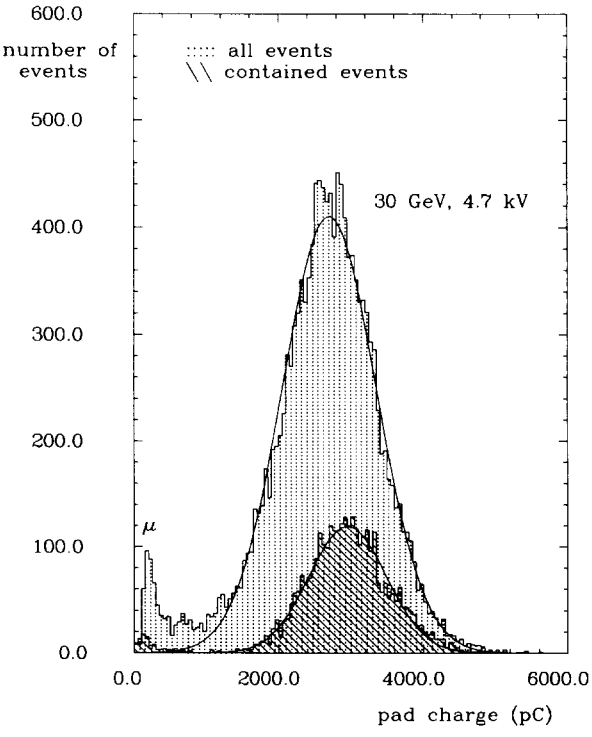

Fig. 12. Charge spectrum for pions at 30 GeV and 4.7 kV obtained with pad readout, for all events and for the fully contained ones, together with a Gaussian fit.

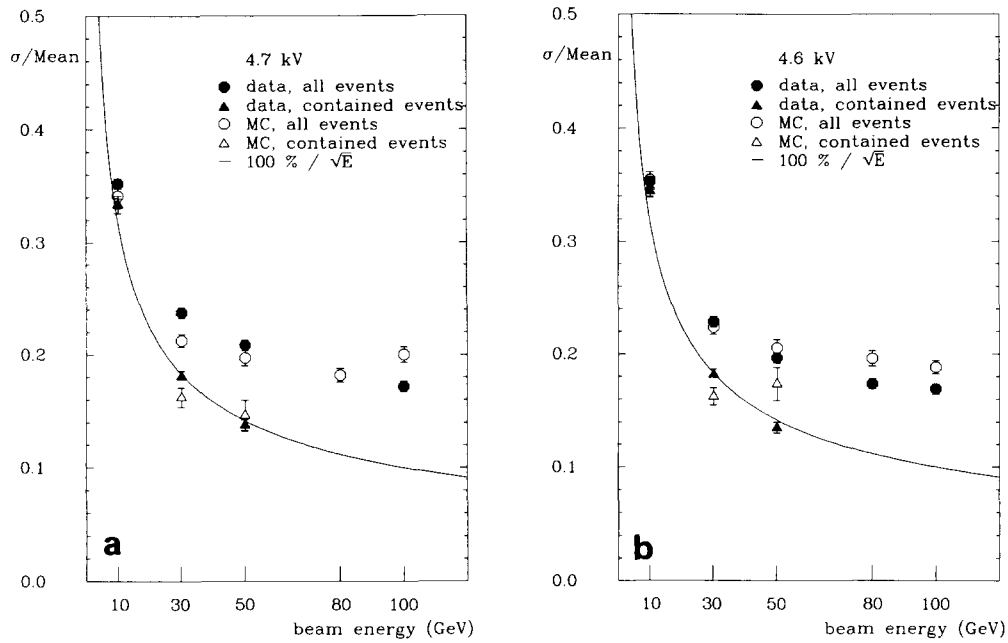

Fig. 13. Charge resolution (pad readout) for pions (data and Monte Carlo, for all events and for the fully contained ones). For the contained events, this corresponds directly to the energy resolution, as the calibration is linear. (a) 4.7 kV, (b) 4.6 kV.

tor the streamer tube calorimeter will serve as "tail catcher" for low energy particles leaking out of the central LAr hadron calorimeter.

The corresponding figures for the 4.6 kV data are shown in figs. 11b (linearity) and 13b (energy resolution). The results are similar to those obtained at a high voltage of 4.7 kV. The absolute calibration is (63.6 ± 0.5) pC/GeV corresponding to 3.9 streamers per GeV.

3.2.3. *Results obtained with the strip readout*

For low energies, the strip multiplicity provides the possibility to measure the energy. Fig. 14 shows the

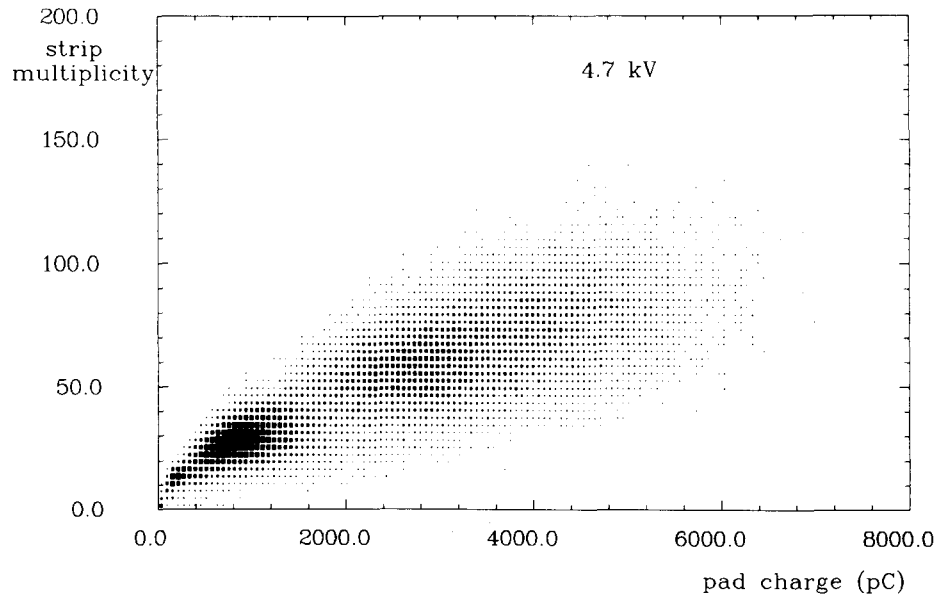

Fig. 14. Pad charge vs multiplicity of parallel strips for pions of 10, 30 and 50 GeV at 4.7 kV (about 10000 events each).

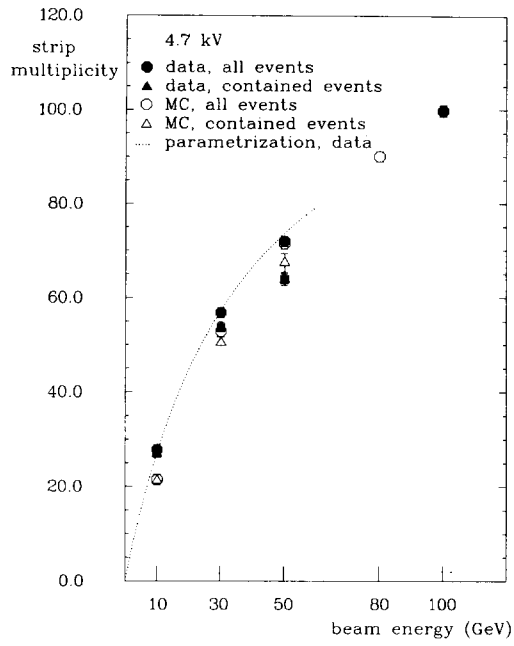

Fig. 15. Strip multiplicity for parallel strips vs beam energy for pions at 4.7 kV (data and Monte Carlo, for all events and for the events fully contained in the calorimeter) together with a parametrization curve.

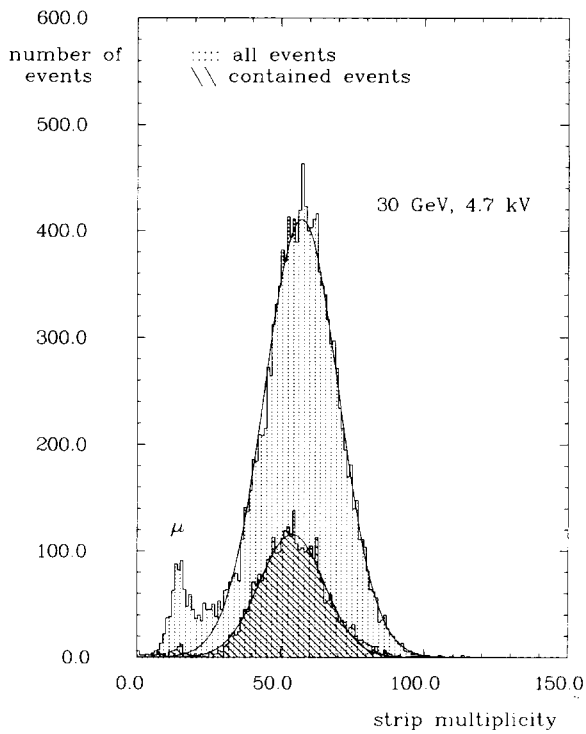

Fig. 16. Strip multiplicity for parallel strips for pions of 30 GeV at 4.7 kV (for all events and the fully contained ones), together with a Gaussian fit.

strip multiplicity (i.e. the total number of parallel strips fired in layers, 1, 4, 5, 6, 7, 8, 9, 10, 11 and 12) plotted versus the charge measured on the pads for each event for 10, 30 and 50 GeV pions. A nonlinear correlation is seen. This nonlinearity can also be seen when plotting the mean strip multiplicity versus the beam energy (see fig. 15). Due to the digital readout of the strips, multiple hits on one wire are invisible (only a projection of the shower is seen). This leads to an early saturation. The measured multiplicity for the contained events (also shown in fig. 15) is lower than for all events, because for contained events the track density inside a shower is higher, leading to a stronger saturation. The multiplicity distributions for 30 GeV pions for all events and for the contained events are shown in fig. 16. Although the spectra are not quite Gaussian, we have calculated the resolution using the same algorithm as for the pad signals (see section 3.2.2). The multiplicity resolutions obtained are shown in fig. 17. They are about constant at ~ 25%. Similar results have been shown in ref. [11]. For the contained events, no improvement is seen. A possible improvement due to missing leakage is spoiled by the stronger saturation.

Since the calibration function is not linear (see fig. 15), the resolution of the strip multiplicity is, however, *not* equal to an energy resolution. If one estimates the energy for each event from the strip multiplicity using the calibration function shown in fig. 15, the energy

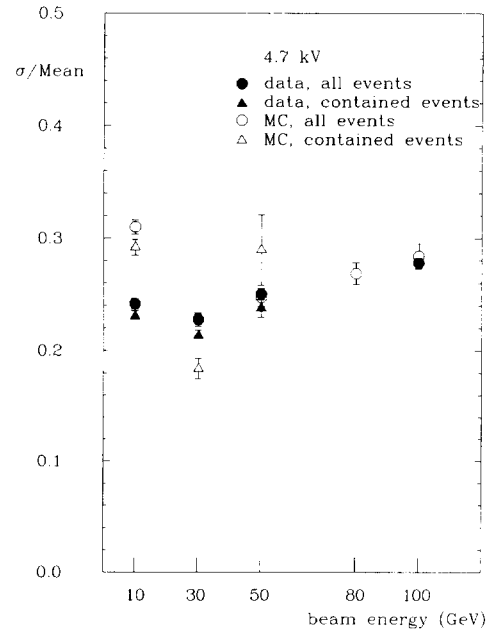

Fig. 17. Multiplicity resolution for pions at 4.7 kV (data and Monte Carlo, for all events and for the fully contained ones).

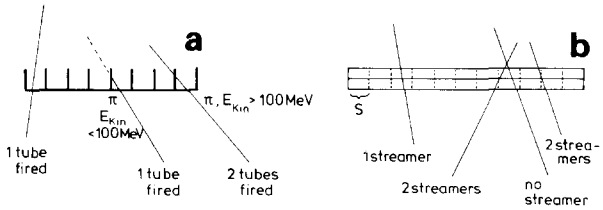

Fig. 18. Simulation of the streamer mode, (a) perpendicular to the wire, (b) in wire direction.

resolution at 10 GeV amounts to $\sigma_E/E = 33\%$ (for the strip multiplicity distribution, the resolution is σ/mean $= 24\%$). This value is comparable to the energy resolution obtained from the pads ($\sigma_E/E = 35\%$). For higher energies, σ_E/E as calculated from the strip multiplicity increases.

3.2.4. Comparison with Monte Carlo simulations

To understand the behaviour of the calorimeter, detailed Monte Carlo (MC) studies have been performed [12]. Hadronic showers were simulated by the GHEISHA code [13] version 7.04. All material except the chamber walls between the wires was included in the shower simulation. The simulation of the streamer mode was performed following an approach given in ref. [14]:

In the plane perpendicular to the wire direction, for all tubes (active size 9×9 mm^2, wire distance 1 cm within one tube element and 1.4 cm between adjacent tube elements) which were hit by a charged particle at least one streamer was generated. Particles which only hit the inactive walls were not accepted. Particles which hit two or more adjacent tubes were only allowed to set more than one hit if their kinetic energy exceeded 100 MeV. Otherwise they were regarded as absorbed in the wall and streamers were generated only in the first hit tube (see fig. 18a).

To calculate the number of streamers generated along the wire direction, each tube was divided into predefined cells of a given cell size s. Each cell which was hit by at least one charged particle was regarded as one streamer. Double hits were only counted once. Thus the parameter s is a measure for the size of the dead region around one streamer. Fig. 18b shows an example. This procedure was done for three different values of s: 2, 3 and 5 mm.

The pad signals were given by the total number of streamers within the volume of a tower multiplied by the mean charge per streamer taken from the measurements (see section 3.1.2). Then, a negative crosstalk of -9% of the signal and a cutoff to simulate ADC overflows was applied. The absolute calibration value obtained for the MC was 4.8 (4.0, 2.9) streamers per GeV incident energy for $s = 2$ mm (3 mm, 5 mm) compared to 4.3 streamers per GeV obtained for the data. This indicates a best value of s of about 2.6 mm (this is in good agreement with measurements of the dead zone around a streamer given in ref. [15]). For the energy resolution, best agreement between data and MC is found for $s = 3$ mm. All further figures are shown for $s = 3$ mm. Linearity curve and energy resolution for the MC are shown in figs. 11c and 13a. Both agree well with the data. To simulate the 4.6 kV data, only 91% of the generated streamers were accepted (as indicated by the reduced absolute calibration). The resolutions obtained are comparable to the ones obtained for the 4.7 kV simulation (see fig. 13b).

For the simulation of the strip response, a variable number of strips according to the measured multiplicity distribution for muons (see section 3.1.2) was generated for each streamer. The efficiency for at least one fired strip per streamer was assumed to be 1.00 for the simulation of the 4.7 kV data (the geometric inefficiency has already been treated within the streamer simulation). The mean multiplicities and the resolutions are shown in figs. 15 and 17, respectively. The data agree well with the MC both in multiplicity and resolution, except at 10 GeV where the MC multiplicity is 23% too low and the resolution is too bad. A possible explanation may be that the crosstalk on the strips within a hadronic shower is larger than for muons as (1) the tracks within a shower are generally not perpendicular to the chamber plane and (2) heavy ionizing particles may generate a larger strip multiplicity than minimum ionizing particles. At higher energies these effects become less important because they are partly compensated by saturation effects.

4. Conclusions

Calorimetric measurements with a 4.5λ long iron streamer tube calorimeter with 7.5 cm iron sampling have been performed using pions in the energy range from 10 to 100 GeV for analogue pad readout and digital strip readout. For fully contained events, an absolute calibration of 4.3 streamers per GeV and an energy resolution of about $100\%/\sqrt{E}$ using pad readout has been obtained up to 50 GeV, whereas the resolution decreases slower than $\sim 1/\sqrt{E}$ if events with leakage are included. At lower energies, it is possible to use the digital readout of the strips for energy measurement. At 10 GeV, the energy resolution obtained with the strips is compareable to the one obtained with the pads. The measurements are in good agreement with Monte Carlo calculations.

Acknowledgement

We gratefully acknowledge the help of the technicians and engineers of the collaborating institutes, par-

ticularly B. Debye, M. Dohmen, P. Keutzer, and R. Siedling from Aachen and U. Dretzler, G. Ernst, N. Koch, G. Metze, P. Vaupel and K. Widynski from Dortmund. We would also like to thank P. Laurelli, P. Massera, P. Picchi, G. Polgrossi and M. Spinetti for support during the chamber production. Finally, we would like to thank the CERN SPS machine group for the operation of the SPS and the H6 beam line and the CERN directorate for the hospitality extended to us during our stay at CERN.

References

[1] H1 Collaboration, Ch. Berger et al., Technical Proposal for the H1 Detector, Hamburg (1986) unpublished.
[2] H1 Collaboration, W. Braunschweig et al., DESY 87-098 (1987) submitted to Nucl. Instr. and Meth.
[3] H1 Collaboration, Detailed Calorimeter Test Results, in preparation.
[4] H6 Beam Tuning, CERN/SPS/EPB/PC (1981).
[5] P. Coet, CERN/SPS 85-14 (1985).
[6] C. Bovet et al., CERN/SPS 82-13 (1982).
[7] E. Iarocci, Nucl. Instr. and Meth. 217 (1983) 30.
[8] G. Battistoni et al., Nucl. Instr. and Meth. 217 (1983) 429.
[9] G. Battistoni et al., Nucl. Instr. and Meth. A251 (1986) 286.
[10] S. Brinkman, Diplom Thesis, Dortmund (1988) in preparation.
[11] M.G. Catanesi et al., Nucl. Instr. and Meth. A247 (1986) 438.
[12] E. Vogel, Thesis, Aachen (1988) in preparation.
[13] H. Fesefeldt, PITHA 85/02, Aachen (1985).
[14] B. Bleichert et al., Nucl. Instr. and Meth. A241 (1985) 43.
[15] G.D. Alekseev et al., Nucl. Instr. and Meth. 177 (1980) 385.